Journal of Alloys and Compounds 817 (2020) 152807

Contents lists available at ScienceDirect

Journal of Alloys and Compounds

journal homepage: http://www.elsevier.com/locate/jalcom

On the grain refining efficacy of Ti-free hypoeutectic AlSi via AlTiB, AlB and AlNbB chemical inoculation

Leandro Bolzoni [a, b, *], Nadendla Hari Babu [b]

[a] School of Engineering, The University of Waikato, Private Bag 3105, Hamilton, 3240, New Zealand
[b] BCAST, Brunel University, Kingston Lane, Uxbridge, Middlesex, UB8 3PH, United Kingdom

ARTICLE INFO

Article history:
Received 2 September 2019
Received in revised form
24 October 2019
Accepted 25 October 2019
Available online 31 October 2019

Keywords:
Aluminium alloys
Grain refinement
Heterogeneous nucleation
Solidification microstructure
Nb–B inoculation

ABSTRACT

Metals with a fine grain structure have intrinsic advantages like higher mechanical strength and more isotropic behaviour. An effective way of refining the grain size is via chemical inoculation. In this study the grain refining efficacy of AlTiB, AlB and AlNbB master alloys on a Ti-free AlSi alloy is investigated. In particular, the performance of commercial Al5Ti1B and Al5B master alloys is compared to that of a lab-made Al2Nb2B and two Al2NbxB (x = 1 and 2 wt%) made in an industrial pilot scale facility. Although chemical inoculation does not change the morphology of the grains, which is always equiaxed dendritic, it is found that the grain size progressively decreases with the master alloy addition rate and the achievable final grain size is strongly dependent on the chemistry of the master alloy used. The experimental results demonstrate that AlNbB > AlB > AlTiB in terms of grain refining efficacy.

1. Introduction

The grain refinement of light alloys via chemical inoculation, for example wrought Al alloys by means AlTiB master alloys, has been extensively studied over the last decades aiming to comprehend the mechanism governing the grain refinement and optimise the inoculation process for its industrial use as well as to develop new grain refining compositions [1–3]. AlTiB master alloys have lower grain refining ability in foundry alloys, such as AlSi alloys with Si > 3% (compositions are in wt.% if not specified differently), as the potency of the Ti-based particles is annihilated by the presence of Si, a phenomenon known as poisoning [4–8]. The use of AlB (i.e. B-based) master alloys to reduce Si poisoning and achieve grain refinement of foundry AlSi alloys was analysed by Wu et al. [9] in the 1980s. Chemical inoculation of AlSi alloys by means of AlB master alloys has received renewed attention by the scientific community in recent years aiming to understand the potency of AlB master alloys, both in pure Al [10] and foundry AlSi alloys [11], and clarify the mechanism governing the refinement [12].

It is worth noting that most of the studies performed on the subject were done using commercially pure Al and high purity Si to manufacture the foundry AlSi alloys to be grain refined and, thus, AlB master alloys showed good efficacy. However, when AlB master alloys are used to inoculate commercial foundry AlSi alloys they are less effective and their grain refining ability fades with the contact time (i.e. the time after the initial chemical inoculation). The critical difference between lab-made AlSi and commercial foundry AlSi alloys is that the former are Ti-free whereas in the majority of the cases the latter contain Ti (max ~0.1%), either present as impurity or intentionally added as most foundries still use Ti-based master alloys in their cast. Birol [11,13] reported that AlB master alloys have similar behaviour to that of AlTiB master alloys when the former are used to inoculate commercial foundry AlSi alloys. Reason behind being the fact that, thermodynamically, Ti boride is more stable than Al borides [14] and thus, over time, the latter will transform into the former if Ti is present.

Over the last lustre, the authors of this manuscript have proposed the use of Nb–B inoculation presenting evidences of its efficacy in binary and commercial AlSi alloys [15,16] where many of these first developments were done using Nb powder and KBF_4 [17]. Due to the poor Nb and B yield of recovery achieved when adding Nb powder and KBF_4, we then focused on preparing effective AlNbB master alloys that could efficiently refine commercial foundry AlSi alloys [15,16] and permitted to obtain equiaxed-grain structures in direct chilled (DC)-casting billets [18]. For that the master alloys were manufactured using an Al5B master alloys as

* Corresponding author. School of Engineering, The University of Waikato, Private Bag 3105, Hamilton, 3240, New Zealand.
E-mail address: leandro.bolzoni@gmail.com (L. Bolzoni).

https://doi.org/10.1016/j.jallcom.2019.152807

source of B and with an improved way of prevent oxidation of Nb during its addition to the molten Al. The next natural stage was to move the production of AlNbB master alloys at industrial level, test their performance, and understand their grain refining efficacy. The aim of this work is then to present and discuss the grain refining efficacy of industrially produced AlNbB master alloys. From literature on the subject it is clear that variations in impurity level of the alloys used and in solidification conditions affect the final results, making the comparison among works performed in different institutions unreliable. Therefore, in this study the same AlSi alloys is chemically inoculated with different potential refiners including commercial Al5Ti1B and Al5B master alloys and a lab-made Al2Nb2B master alloy along with industrially produced Al2NbxB master alloys, where x = 1 and 2.

2. Experimental procedure

Commercial pure (CP) Al (99.8% purity) and the Al5Ti1B and Al5B master alloys are commercial products so no much characterisation was performed on them if not confirming that the Al5B master alloy contains Al borides (i.e. AlB_2 and AlB_{12}). The lab-made Al2Nb2B master alloy was produced by melting CP Al at 790 °C during 1 h to which the Al5B master alloy and Nb powder were added. For that the temperature was raised to 850 °C and the chemical elements left to dissolve during 3 h with intermediate manual stirring [18]. Industrially manufactured Al2NbxB master alloys (labelled as IM-Al2Nb1B and IM-Al2Nb2B) were made mixing CP Al, an Al7Nb master alloy, and potassium tetrafluoroborate KBF_4 using the procedure commonly employed to industrially manufacture AlTiB master alloys. The microstructure of the Al2NbxB master alloys was investigated by SEM using a Zeiss Supra 35VP FEG for phase identification and semiquantitative elemental chemical analysis. An aqueous solution with 15% NaOH was used to deep etch the Al2NbxB master alloys to reveal the 3D morphology of the particles present and their particle size distribution was analysed via SEM micrographs. Phase identification was done via X-ray diffraction on a Bruker AXS D8-Advance analyser equipped with a Cu $K_{\alpha 1}$ radiation monochromator.

Grain refinement experiments were performed on a Ti-free Al9.9Si0.1Fe alloy via chemical inoculation with the different master alloys considering addition rates of 0.025–0.2%. The chemical composition of the reference alloy and of the master alloys is shown in Table 1. It is worth mentioning that, due to limitations of lab based equipment, the actual composition of the Al2NbxB master alloy, especially the lab-made, is expected to be lower than the nominal composition. Consequently, the addition rates are identified as *nominal*.

Reference samples were also cast under the same conditions for the sake of comparison of the grain structure before and after chemical inoculation, which was performed at 740 °C. In particular, batches of 500 g of the alloys were considered. The inoculated Al9.9Si0.1Fe alloy was stirred after the master alloys were added and left to repose for 30 min of contact time. The alloys were cast into a cone-shaped (max ⌀68 mm × 90 mm) preheated steel mould with a mean cooling rate of 0.5 °C/s as previously measured with K-type thermocouple [19]. The summary of the conditions tested is reported in Table 2. The experiments were designed in terms of wt.% of the principal alloying element of the master alloy rather than addition rate of the master alloy itself in order to be able to carry out multiple comparisons. Some of those are straightforward such as 0.1% of Ti, B and Nb, and some other inferred such as the addition of 0.1%Ti of the Al5Ti1B master alloy is equivalent to 0.02% B which is comparable to the addition of 0.025%B via the Al5B master alloy.

The cast samples were cut in two halves for metallographic analysis. For both macro- and microanalysis the samples were prepared using a standard metallographic procedure but finally etched using Tucker's (15 ml HF + 15 ml HNO_3 + 45 ml HCl + 25 ml H_2O) and Barker's (4 mL of HBF_4 in 100 mL of H_2O) solutions, respectively. A Zeiss Axioscope microscope was used to take the light polarised optical micrographs then employed for grain size measurements performed as per the linear intercept method (ASTM E112-10). It is worth mentioning that ten different light polarised optical micrographs were used for each alloy to generate the data for the calculation of the average and the variation of the grain size.

3. Results and discussion

3.1. Features of the AlNbB master alloys

From the characterisation of the lab-made Al2Nb2B master alloys, a uniform distribution of particles (approximately 0.5–10 μm) embedded into the Al matrix is found as visible from the optical micrograph shown in Fig. 1a. Few B-rich particles (i.e. AlB_x) and copious Nb-based compounds particles (i.e. hexagonal platelets NbB_2 and blocky Al_3Nb) are found in the SEM micrographs of the Al2Nb2B master alloy (Fig. 1b and d) where deep etching of the master alloy reveals that both individual particles (Fig. 1c) and clusters of particles (Fig. 1e) of Nb-based compounds are present. The agglomerated particles are a consequence of the production route used as the master alloy was stirred to solidification [18] and will dissolve once added to the molten metal. The XRD patter of Fig. 1f), which is representative for all the Al2NbxB master alloys regardless of their manufacturing route, confirms the phase identified via microstructural analysis.

In the case of the IM-Al2NbxB master alloys, the Nb-based particles exhibit ring-like clusters (Fig. 2a). It is worth mentioning that these master alloys also have Al borides particles. Moreover, some residue from the use of KBF_4 as source of B are also found (Fig. 2b). The particle size is within the 1–7 μm range. Comparable particle size range (0.2–6 μm) was reported for the commercial Al5Ti1B master alloys and as per the free growth model proposed by Greer et al. [20] the particles with a diameter greater than 3 μm

Table 1
Nominal chemical composition of the inoculated alloys and of the master alloys used for inoculation.

	Element [wt.%]					
	Si	*Fe*	*Ti*	*Nb*	*B*	*Al*
Reference	9.9	0.1	-	-	-	Balance
Al5Ti1B	-	-	5.0	-	1.0	Balance
Al5B	-	-	-	-	5.0	Balance
Al2Nb2B	-	-	-	2.0	2.0	Balance
IM-Al2Nb1B	-	-	-	2.0	1.0	Balance
IM-Al2Nb2B	-	-	-	2.0	2.0	Balance

Table 2
Details of the inoculation experiments performed. Note: the equivalent B addition rate is reported between brackets.

Inoculation addition rate (equivalent B) [wt.%]				
	0.025	*0.05*	*0.1*	*0.2*
Al5Ti1B	-	-	Ti (0.02)	Ti (0.04)
Al5B	B (0.025)	B (0.5)	B (0.1)	-
Al2Nb2B	Nb (0.025)	Nb (0.5)	Nb (0.1)	-
IM-Al2Nb1B	-	Nb (0.025)	Nb (0.05)	-
IM-Al2Nb2B	-	Nb (0.05)	Nb (0.1)	-

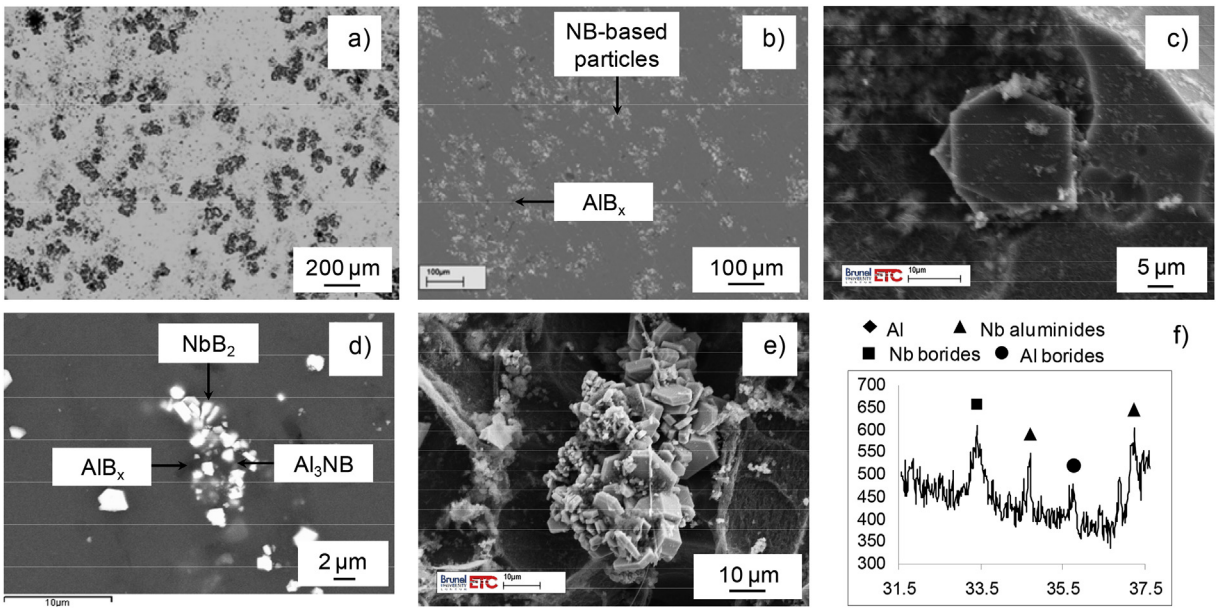

Fig. 1. Microstructural characterisation of the lab-made Al2Nb2B master alloy: (a) optical micrograph of the distribution of the inoculating particles; polished and deep-etched, respectively, SEM micrographs showing (b–c) individual particles and (d–e) clusters of particles; and (f) XRD of the phases present.

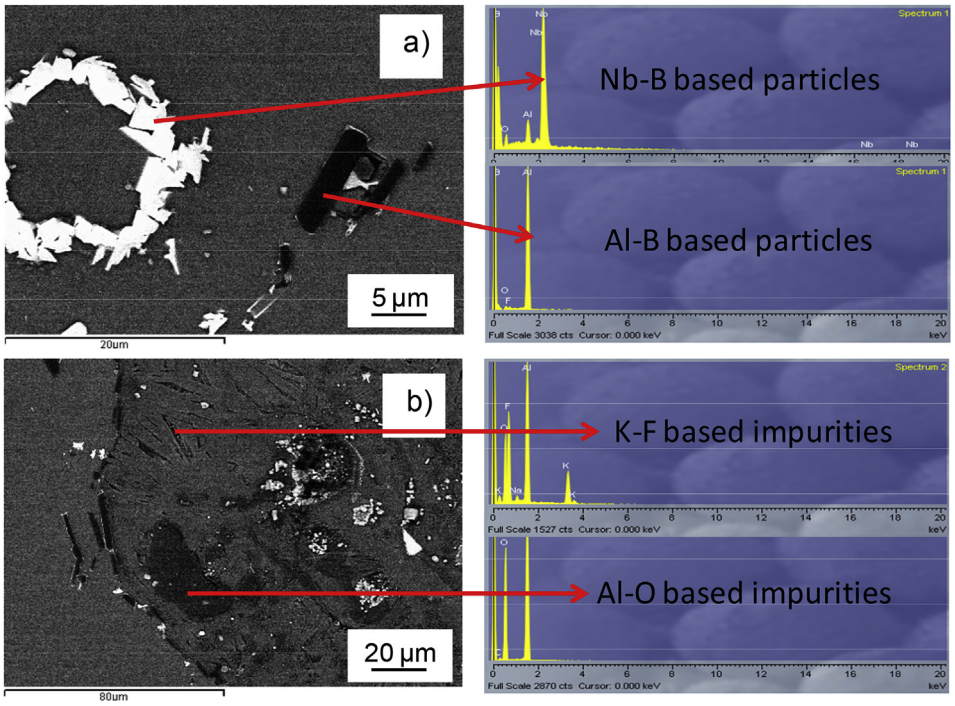

Fig. 2. Detail of the Nb-based ring-like clusters (a), and KBF_4 residue (b) of the industrially produced AlNbB master alloys (i.e. IM-Al2NbxB).

are to one most likely to be active as heterogeneous nucleation substrates under typical Al foundry casting conditions.

3.2. Al9.9Si0.1Fe alloy

Cast CP Al has a microstructure predominantly composed of columnar grains [12] but the presence of Si, as low as 1%, as alloying element changes the morphology of the grain to equiaxed dendritic. The switch of the growing mode from planar to dendritic is due to the partioning effect of Si, quantifiable via the growth restriction factor as $Q = C_o \cdot 5.9$ (where C_o is the nominal composition of the allotting element), and it is associated to a reduction in grain size. As repeatedly reported in the literature [4,8,21–23], the grain size will continue to decrease with the Si content but starting from ~3 to 4%Si will start to increase again. Fig. 3 shows the as-cast macrostructure and microstructure of the Al9.9Si0.1Fe alloy without inoculation.

The alloy shows the typical cast macrostructure composed of three regions: (1) fine equiaxed grains in the surface as a result of the fast heat exchange when first in contact with the preheated

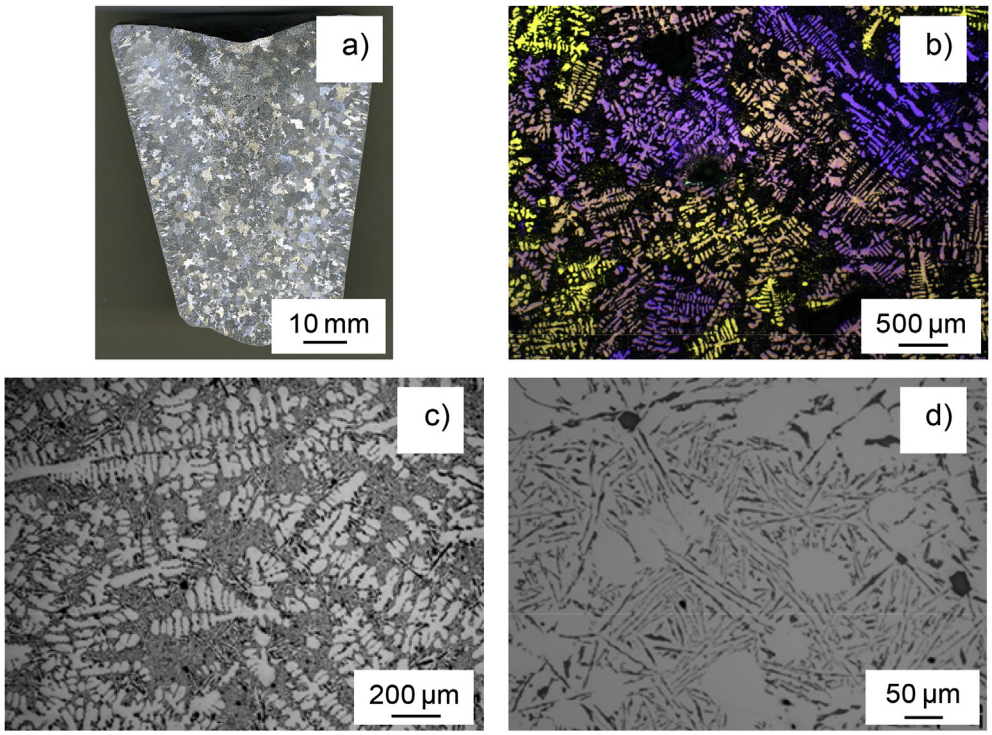

Fig. 3. Macrostructure (a), microstructure (b-c), and detail of the secondary phases (d) of the Al9.9Si0.1Fe alloy solidified with a cooling rate of 0.5 °C/s from 740 °C.

mould; (2) columnar grains grew in the opposite direction of the latent heat extraction direction; and (3) equiaxed dendritic grains in the core of the casting due to the partioning of Si and its related grow restriction. This difference in grain morphology and size affects the response of the alloy to any potential heat treatment or thermomechanical process to be applied to tailor the mechanical behaviour [1,2,24,25]. For example, longer solution times are required during a T6 heat treatment highlighting one of the benefit and need of achieving a fine homogeneous as-cast grain structure. Grain size measurements were done on light polarised micrographs where primary α-Al equiaxed dendritic grains are present such as the example shown in Fig. 3b. As per the binary AlSi phase diagram [26–28], the eutectic composition is 12.6% Si. However, the partitioning of Si during non equilibrium solidification leads to the nucleation of secondary eutectic Si phase and primary Si particles. The former appears as needles in 2D micrographs (in reality faceted 3D plate-like flakes [29,30]) whereas the latter are polyhedral particles in 2D micrographs, in fact faceted blocky 3D crystals. Both phases are found between the primary and secondary arms of the α-Al dendrites which is where the rejected Si is accumulated upon solidification (Fig. 3d).

3.3. Inoculation via Al5Ti1B master alloy

Inoculation of the Al9.9Si0.1Fe alloy by means of the Al5Ti1B master alloys does not change the structure of the cast alloy if not that the grain size is somewhat smaller (Fig. 4). The addition of AlTiB master alloys cannot suppress the formation of columnar grains, which are still present in the surface of the casting (Fig. 4a), and does not change the morphology of the main microconstituents: equiaxed dendritic grains (Fig. 4b). Lastly, the AlTiB inoculated Al9.9Si0.1Fe alloy is still characterised by the presence of the needle-like eutectic phase and of polyhedral primary Si particles. No remarkable difference in terms of distribution, size and morphology of these secondary phases in comparison to the Al9.9Si0.1Fe alloy can be highlighted from the microstructure analysis (Fig. 4d). This is in agreement with current literature showing that chemical inoculation via AlTiB master alloys does not affect the size and shape of secondary phases.

3.4. Inoculation via Al5B master alloy

Results of the characterisation of the Al9.9Si0.1Fe alloy inoculated using the commercial Al5B master alloy are shown in Fig. 5. It is found that AlB inoculation cannot completely prevent the formation of columnar grains near the edge of the casting (Fig. 5a) but the width of the band where columnar grains are present is smaller with respect to both the Al9.9Si0.1Fe alloy without (Fig. 3a) and with Al5Ti1B inoculation (Fig. 4a). The microconstituents of the inoculated alloy remain secondary plate-like eutectic and blocky primary Si particles (Fig. 5d) entrapped between the arms of the primary α-Al equiaxed dendritic grains (Fig. 5b). Once again no significant differences are found for the former with respect to the previous discussed experiments but the latter are finer as a result of the finer primary α-Al equiaxed dendritic grains.

3.5. Inoculation via Al2NbxB master alloys

It is found that the main effects of inoculating the Al9.9Si0.1Fe alloy via Al2NbxB master alloys are always the same, regardless of how the master alloys were produced, and therefore the results are discussed altogether. Firstly, no band of columnar grains is present in the castings inoculated with Al2NbxB master alloys (Fig. 6a and b) consistently with our previous results on the formation of equiaxed structures in directionally solidified DC-casting billets [18]. Secondly, the morphology of the equiaxed dendritic grains is not changed but, generally, their size is notably smaller (Fig. 6c-f). Finally, the features of the secondary phases (i.e. eutectic Si and primary Si particles) are also affected achieving a much more uniform distribution of finer 2D needle-like and much fewer and

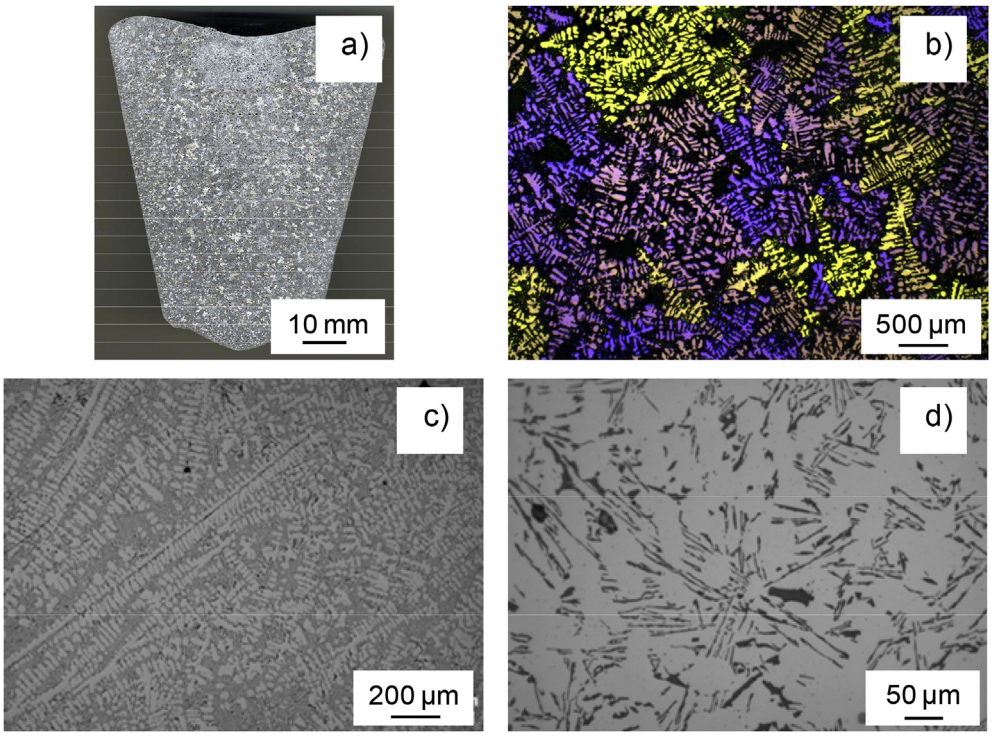

Fig. 4. Macrostructure (a), microstructure (b-c), and detail of the secondary phases (d) of the Al9.9Si0.1Fe alloy inoculated with the Al5Ti1B master alloy.

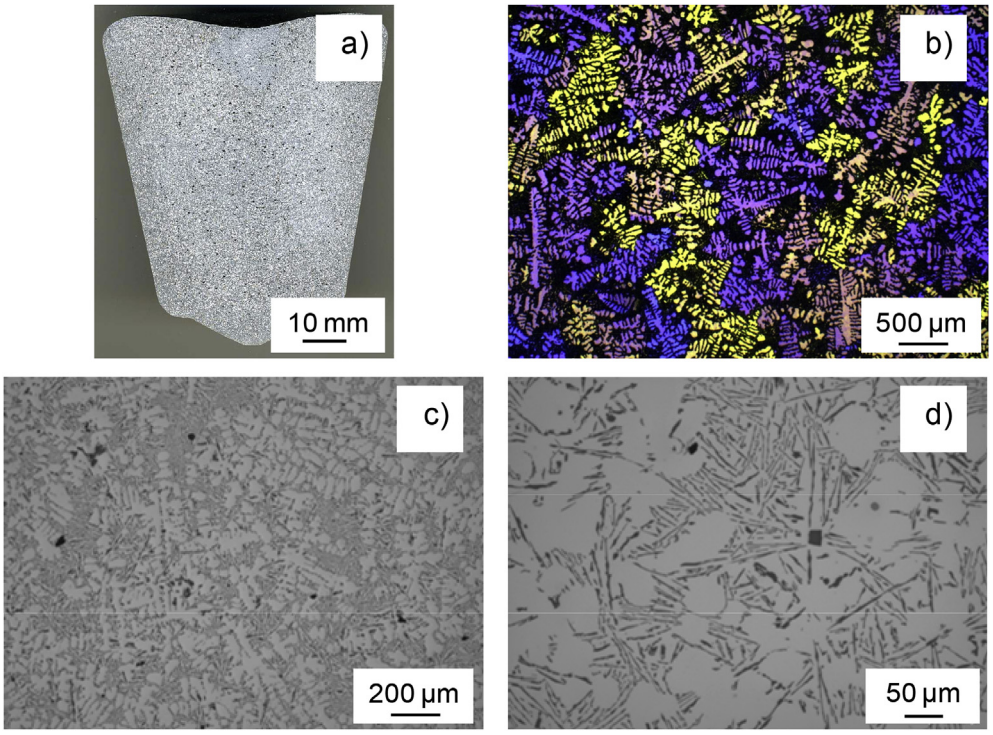

Fig. 5. Macrostructure (a), microstructure (b-c), and detail of the secondary phases (d) of the Al9.9Si0.1Fe alloy inoculated with the Al5B master alloy.

smaller polyhedral primary Si particles (Fig. 6g-h). Changes of the characteristics of the secondary phases of the Al9.9Si0.1Fe alloy is a spillover benefit of the presence of a much greater number of primary α-Al grains leading to a more uniform accumulation and redistribution of Si atoms in front of the growing grains and in the remaining molten pools as the added Nb-based heterogeneous substrates do not have the right features (i.e. lattice and lattice mismatch) to promote the nucleation of Si.

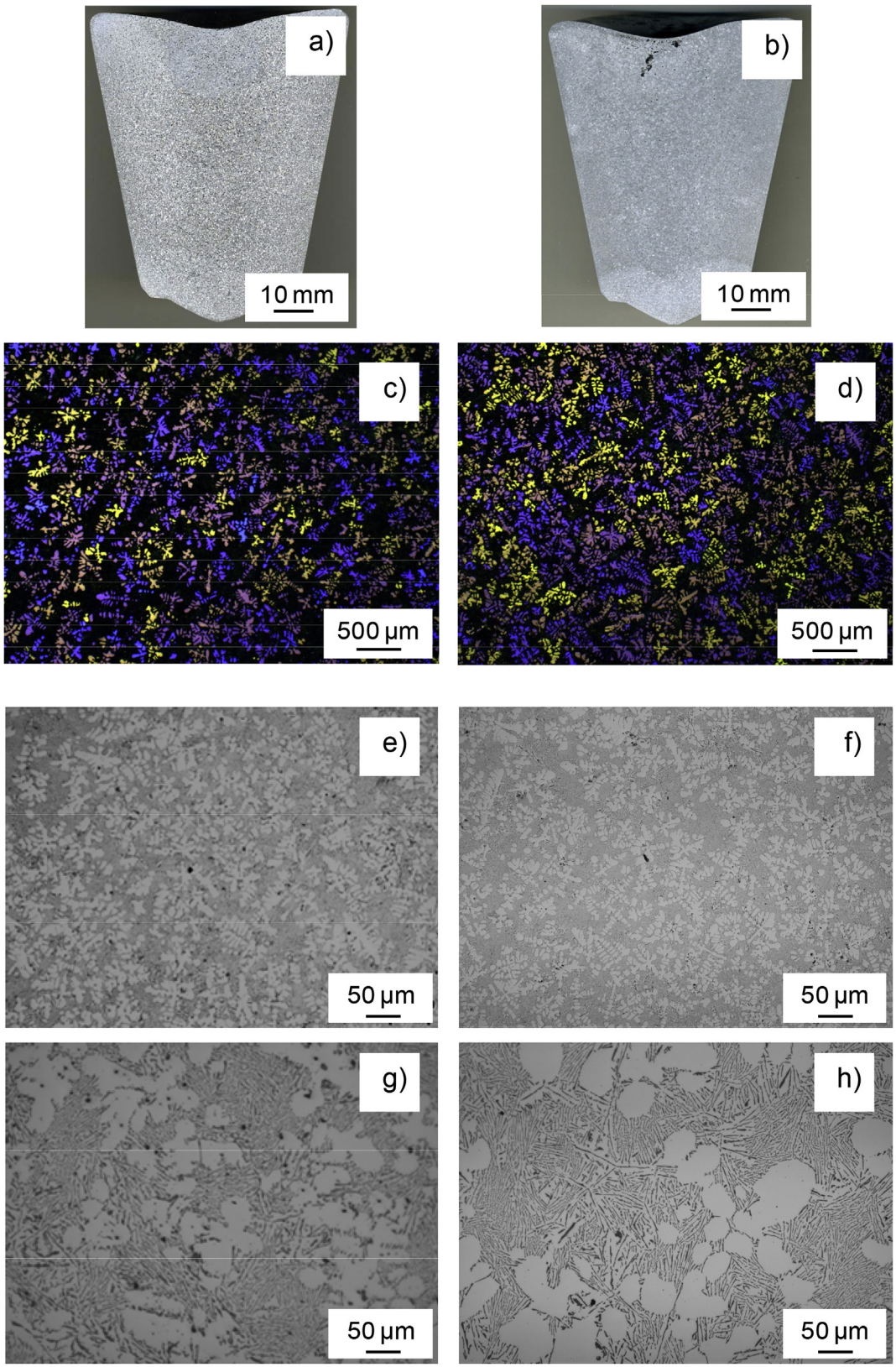

Fig. 6. Macrostructure (a–b), microstructure (c-f), and detail of the secondary phases (g-h) of the Al9.9Si0.1Fe alloy inoculated with the lab-made and industrially manufactured Al2NbxB master alloys, respectively.

3.6. Comparison of the grain refinement

The grain size of the Al9.9Si0.1Fe alloy, taken as reference (Fig. 3b), is 1373 ± 170 µm as visible in Fig. 7 which shows the variation of the grain size versus the *nominal* addition rate for the different sources of chemical inoculation studied. In the case of the

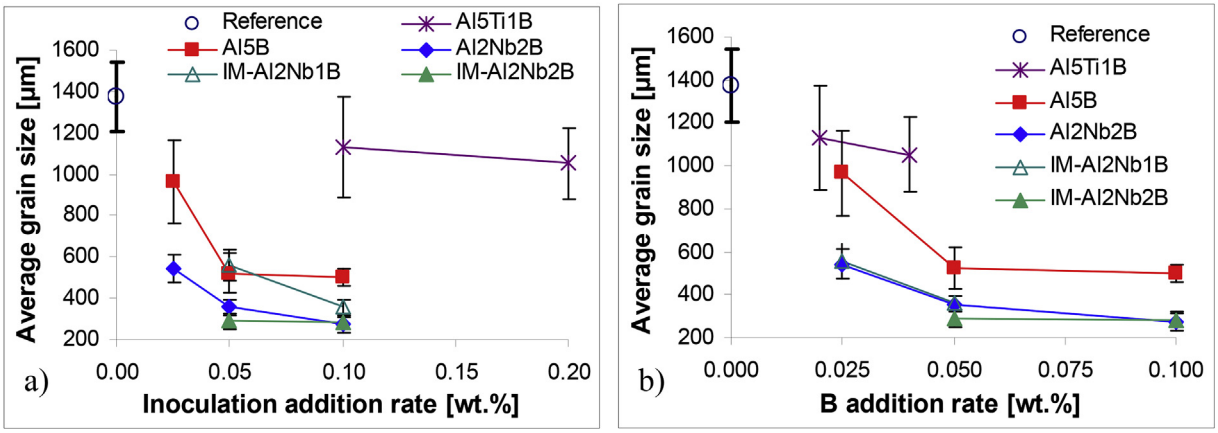

Fig. 7. Variation of the grain size of the Al9.9Si0.1Fe alloy versus *nominal* inoculation addition rate for commercial Al5Ti1B and Al5B master alloys and lab-made Al–Nb2B and industrially made IM-Al2Nb1B and IM-Al2Nb2B master alloys: a) average grain size vs. *nominal* inoculation addition rate, and b) average grain size vs. *nominal* B addition rate.

commercial Al5Ti1B master alloy, the chosen addition rate (up to 0.2% Ti) is higher in comparison to the standard used in industry to inoculate wrought Al alloys (0.005–0.10% Ti). Despite that, the grain size of the Al9.9Si0.1Fe alloy is only progressively refined down to around 1100 µm which is consistent with values of grain size (~1400 µm) found in the literature for the inoculation of a lab-made binary Al10Si alloy with 0.05% Ti [31]. Due to the coarse dendritic structure it can also be noticed that there is quite a significant variance of the data.

The average grain size is progressively refined with the addition rate when the Al9.9Si0.1Fe alloy is inoculated with the commercial Al5B master alloy. However, no much further refinement is obtained when increasing the addition rate from 0.05% to 0.1% (Fig. 7a) as the grain size is still approximately 500 µm. A continuous refinement of the grain size is obtained via inoculation by means of Al2NbxB master alloys. From Fig. 7a), the smallest grain size is achieved when using Al2Nb2B with a *nominal* addition rate of 0.1% Nb although the improvement obtained when increasing the addition rate from 0.05% to 0.1% is only marginal for the IM-Al2Nb2B master alloy, and somewhat more pronounced (~70 µm) for the lab-made Al2Nb2B master alloy, respectively. The efficacy of the different chemical inoculation analysed can thus be described in the following decreasing order AlNbB > AlB > AlTiB.

Spittle [22,23] reported that confusion and misleading statements happen as investigators have frequently attempted to compare the grain refining efficiencies of alternatives such as AlB, AlTiC and AlTiB with Ti/B < 2.2:1 with traditional refiners. The main cause being that significant level of residual Ti could mask the true effect of the refiner. More reliable results are supposed to be obtained if the comparison is done on the basis of a common elements, B in most instances. The results of the refinement of the Al9.9Si0.1Fe alloy plotted against the *nominal* B% are shown in Fig. 7b). As the Al9.9Si0.1Fe alloy considered in this study is Ti-free, the order of the efficacy of the different master alloys is not altered (i.e. AlNbB > AlB > AlTiB). However, it can be noticed that the low addition rate the Al5Ti1B master alloy (0.02% B) has comparable refinement to that of the Al5B master alloy (0.025% B). Moreover, it is worth noticing that the grain refinement attained with IM-Al2Nb1B master alloy is similar to that of the Al2Nb2b master alloys, which could not be pointed out from Fig. 7a). This confirms that, as previously reported [32], a high amount of B is not needed in Al2NbxB master alloys, and with an optimised industrial production route, lower B in the master alloys and lower addition rates could be used.

Since the very early studies about grain refinement performed by Cibula [33,34], a significant parameter is the potency of the substrate. Among the different factors that are thought to control the efficacy of grain refinement such as contact angle [35], size of the nucleants [20], and interaction of the nucleants with the alloy chemistry [36], the crystallographic matching between the nucleants and the matrix is considered to be critical. Good crystallographic matching favours the formation of interfaces with low energy which normally happens along particular lattice directions and planes and, therefore, particular orientation relationship (*OR*) can be identified. The interatomic spacing misfit (f_r), and the interplanar spacing mismatch (f_d) associated with each potential *OR* can then be calculated. f_r and f_d are quantified as the ratio between the difference in lattice parameters or spacing, respectively,

Table 3
Most favourable orientation relationship (*OR*), interatomic spacing misfit (f_r), and interplanar spacing mismatch (f_d) between Al and the heterogeneous nucleation substrates.

Element	Phase	Lattice structure	Orientation relationship (*OR*)	f_r [%]	f_d [%]
Al	Al	FCC	-	-	-
Ti	Al_3Ti [37]	Tetragonal	$\{112\}Al_3Ti//\{111\}Al\ <201>Al_3Ti//<110>Al$	-0.7	1.6
	TiB_2 [37]	HCP	$\{10\bar{1}1\}TiB_2//\{200\}Al\ <11\bar{2}0>TiB_2//<110>Al$	-6.1	-0.9
	Ti_5Si_3 [5]	HCP	$\{112\}Al_3Ti//\{03\bar{3}0\}Ti_5Si_3\ <110>Al_3Ti//<0001>Ti_5Si_3$	5.85	7
			$\{03\bar{3}0\}Ti_5Si_3//\{111\}Al\ <0001>Ti_5Si_3//<110>Al$	11.25	8.65
B	AlB_2 [12]	HCP	$\{10\bar{1}1\}AlB_2//\{220\}Al\ <11\bar{2}0>AlB_2//<110>Al$	-5.1	-0.6
Si	SiB_6 [12]	Cubic	$\{110\}SiB_6//\{220\}Al\ <100>SiB_6//<100>Al$	2.2	2.3
Nb	Al_3Nb [38]	Tetragonal	$\{112\}Al_3Nb//\{111\}Al\ <021>Al_3Nb//<110>Al$	0.7	1.8
	NbB_2	HCP	$\{10\bar{1}1\}NbB_2//\{200\}Al\ <11\bar{2}0>NbB_2//<110>Al$	-8.3	-0.9

and the lattice parameter/spacing of the Al matrix with respect to the heterogeneous nucleation substrates along a particular *OR*. The details of the most favourable *OR* and lowest f_r and f_d values relevant for this work are reported in Table 3.

The data presented in Fig. 7 seems to disagree with the f_r and f_d data reported in Table 3 as nucleation of α-Al grains should be more favourable on TiB_2/Al_3Ti rather than AlB_2/SiB_6. Specifically, it is believed that a thin layer of Al_3Ti is needed and forms on top the TiB_2 (which are the nucleants) during the heterogeneous nucleation of α-Al grains [39]. Similarly, it has been reported that, when Si is present, a SiB_6 layer forms on the surface of AlB_2 particles and this leads to a more efficient nucleation of α-Al grains [12]. However, Qiu et al. [5] reported that, of all the possible titanium silicides phases that can form due to poisoning, Ti_5Si_3 is the one most likely forming. Ti_5Si_3 has the smallest interatomic spacing and interplanar spacing misfits with Al_3Ti, rather than with TiB_2, and would thus form on top of the Al_3Ti layer present on the surface of TiB_2 particles. From Table 3, it can be seen that Ti_5Si_3, which is the lattice crystal from which α-Al grains have to nucleate in the case of Al5Ti1B inoculation, has very poor lattice match with the lattice of Al. Therefore, linear correlations are found between the achievable grain size and f_r and f_d if the phase that is actually in contact with molten Al, and that would nucleate α-Al grains (i.e. Ti_5Si_3) is considered.

4. Conclusions

From this comparative study on the efficacy of different chemical inoculation master alloys to refine the grain structure of Ti-free hypoeutectic AlSi alloys it can be concluded that AlNbB is more effective than AlB which, in turns, is better than AlTiB. Ti-free hypoeutectic AlSi alloys solidified under standard foundry conditions are characterised by the three typical grain structures: chilled zone, columnar grains, and equiaxed dendritic structure. The band constituted by columnar grains is not affected by the addition of AlTiB, but it decreases with AlB, and it is not present when AlNbB is used. Moreover, inoculation reduces the size of the equiaxed grains but does not alter their morphology, which remains equiaxed dendritic. For each master alloy chemistry, the higher the addition rate the finer the grain size. Al2NbxB master alloys produced using an industrial setup have comparable efficacy to that of the lab-made Al2Nb2B master alloy, highlighting that scaling up of the production of AlNbB master alloys is feasible. Nonetheless, microstructural analysis points out that optimisation of the starting materials and, especially, of the manufacturing parameters needs to be performed to obtain chemically clean and reliable AlNbB master alloys for their use in Al foundries. Investigation of the variation of the grain size on the basis of a common element, rather than the addition rate, points to the fact that master alloys with lower boron content and lower addition rates could be used once the industrial production of AlNbB master alloys has been improved and optimised.

Data availability

All metadata pertaining to this work can be accessed via the following link: https://doi.org/10.17633/rd.brunel.10117994 (To be added after review)

Declaration of competing interestCOI

The authors declare no competing financial interest.

Acknowledgements

The financial support from the Engineering and Physical Sciences Research Council (EPSRC) through the EP/J013749/1 Project and from the Technology Strategy Board (TSB) through the TSB/101177 Project is acknowledged.

Appendix A. Supplementary data

Supplementary data to this article can be found online at https://doi.org/10.1016/j.jallcom.2019.152807.

References

[1] D.G. McCartney, Grain refining of aluminium and its alloys using inoculants, Int. Mater. Rev. 34 (1989) 247–260.
[2] B.S. Murty, S.A. Kori, M. Chakraborty, Grain refinement of aluminium and its alloys by heterogeneous nucleation and alloying, Int. Mater. Rev. 47 (2002) 3–29.
[3] T.E. Quested, Understanding mechanisms of grain refinement of aluminium alloys by inoculation, Mater. Sci. Technol. 20 (2004) 1357–1369.
[4] M. Johnsson, Influence of Si and Fe on the grain refinement of aluminium, Z. Met. 85 (1994) 781–785.
[5] D. Qiu, J.A. Taylor, M.X. Zhang, P.M. Kelly, A mechanism for the poisoning effect of silicon on the grain refinement of Al-Si alloys, Acta Mater. 55 (2007) 1447–1456.
[6] T.E. Quested, A.T. Dinsdale, A.L. Greer, Thermodynamic evidence for a poisoning mechanism in the Al-Si-Ti system, Mater. Sci. Technol. 22 (2006) 1126–1134.
[7] S.A. Kori, V. Auradi, B.S. Murty, M. Chakraborty, Poisoning and fading mechanism of grain refinement in Al-7Si alloy, Mater. Forum 29 (2005) 387–393.
[8] L. Bäckerud, M. Johnsson, The relative importance of nucleation and growth mechanisms to control grain size in various aluminium alloys, Light Met. (1996) 679–685.
[9] H. Wu, L. Wang, S. Kung, Grain refining in A 356 alloys, J. Chin. Foundryman Assoc. 29 (1981) 10–18.
[10] T. Wang, Z. Chen, H. Fu, J. Xu, Y. Fu, T. Li, Grain refining potency of Al-B master alloy on pure aluminum, Scr. Mater. 64 (2011) 1121–1124.
[11] Y. Birol, AlB3 master alloy to grain refine AlSi10Mg and AlSi12Cu aluminium foundry alloys, J. Alloy. Comp. 513 (2012) 150–153.
[12] Z. Chen, H. Kang, G. Fan, J. Li, Y. Lu, J. Jie, et al., Grain refinement of hypoeutectic Al-Si alloys with B, Acta Mater. 120 (2016) 168–178.
[13] Y. Birol, Performance of AlTi5B1, AlTi3B3 and AlB3 master alloys in refining grain structure of aluminium foundry alloys, Mater. Sci. Technol. 28 (2012) 481–486.
[14] G.P. Jones, J. Pearson, Factors affecting grain refinement of aluminium using Ti and B additives, Metall. Mater. Trans. B 7 (1976) 223–234.
[15] L. Bolzoni, M. Nowak, N. Hari Babu, Assessment of the influence of Al-2Nb-2B master alloy on the grain refinement and properties of LM6 (A413) alloy, Mater. Sci. Eng. A 628 (2015) 230–237.
[16] L. Bolzoni, N. Hari Babu, Engineering the heterogeneous nuclei in Al-Si alloys for solidification control, Appl. Mater. Today 5 (2016/12/01/2016) 255–259.
[17] M. Nowak, W.K. Yeoh, L. Bolzoni, N. Hari Babu, Development of Al-Nb-B master alloys using Nb and KBF4 Powders, Mater. Des. 75 (2015) 40–46.
[18] L. Bolzoni, M. Xia, N. Hari Babu, formation of equiaxed crystal structures in directionally solidified Al-Si alloys using Nb-based heterogeneous nuclei, Sci. Rep. 6 (2016) 39554.
[19] L. Bolzoni, M. Nowak, N. Hari Babu, Grain refining potency of Nb-B inoculation on Al-12Si-0.6Fe-0.5Mn alloy, J. Alloy. Comp. 623 (2015) 79–82.
[20] A.L. Greer, A.M. Bunn, A. Tronche, P.V. Evans, D.J. Bristow, Modelling of inoculation of metallic melts: application to grain refinement of aluminium by Al-Ti-B, Acta Mater. 48 (2000) 2823–2835.
[21] J.A. Spittle, Grain refinement in shape casting of aluminium alloys, Int. J. Cast Metals Res. 19 (2006) 210–222.
[22] J.A. Spittle, Grain refinement in shape casting of aluminium alloys – Part I, Foundry Trade J. (2008) 308–314.
[23] J.A. Spittle, Grain refinement in shape casting of aluminium alloys – Part II, Foundry Trade J. (2008) 335–340.
[24] E.L. Rooy, Aluminum and Aluminum Alloys, Castings, vol. 15, ASM International, Ohio, 1988.
[25] S.A. Kori, B.S. Murty, M. Chakraborty, Development of an efficient grain refiner for Al-7Si alloy and its modification with strontium, Mater. Sci. Eng. A 283 (2000) 94–104.
[26] ASM International, ASM Handbook Volume 03: Alloy Phase Diagrams, ASM International, Ohio, 1992.
[27] T.B. Massalski, J.L. Murray, L.H. Bennett, H. Baker, Binary Alloy Phase Diagrams, first ed., ASM International, 1986.
[28] J.L. Muray, A. J. Mc Alister, The Al-Si (Aluminum-Silicon) system, Bull. Alloy Phase Diagrams 5 (1984) 74–84.
[29] S.-Z. Lu, A. Hellawell, The mechanism of silicon modification in aluminium-silicon alloys: impurity induced twinning, Metall. Mater. Trans. A 18 (1987) 1721–1733.
[30] S.D. McDonald, K. Nogita, A.K. Dahle, Eutectic nucleation in Al-Si alloys, Acta Mater. 52 (2004) 4273–4280.

[31] Y. Birol, A novel Al-Ti-B alloy for grain refining Al-Si foundry alloys, J. Alloy. Comp. 486 (2009) 219–222.
[32] L. Bolzoni, N. Hari Babu, Efficacy of borides in grain refining Al-Si alloys, Metall. Mater. Trans. A 50 (2019) 746–756, 2019/02/01.
[33] A. Cibula, Grain refinement of aluminum alloy casting by additions of titanium and boron, J. Inst. Met. 80 (1951) 1–16.
[34] A. Cibula, R.W. Ruddle, The effect of grain size on the tensile properties of high strength cast aluminum alloys, J. Inst. Met. 76 (1949-1950) 361–376.
[35] D. Turnbull, Theory of catalysis of nucleation by surface patches, Acta Metall. 1 (1953) 8–14.
[36] P. Schumacher, A.L. Greer, J. Worth, P.V. Evans, M.A. Kearns, P. Fisher, et al., New studies of nucleation mechanisms in aluminium alloys: implications for grain refinement practice, Mater. Sci. Technol. 14 (1998/05/01 1998) 394–404.
[37] M.X. Zhang, P.M. Kelly, M.A. Easton, J.A. Taylor, Crystallographic study of grain refinement in aluminum alloys using the edge-to-edge matching model, Acta Mater. 53 (2005) 1427–1438, 2005/03/01.
[38] F. Wang, D. Qiu, Z.-L. Liu, J. Taylor, M. Easton, M.-X. Zhang, Crystallographic Study of Al3Zr and Al3Nb as Grain Refiners for Al Alloys, vol. 24, Transaction of Nonferrous Metals Society of China, 2014, pp. 2034–2040.
[39] B.J. Mc Kay, P. Schumacher, Heterogeneous nucleation mechanisms of TiB_2 particles in Al alloys, in: TMS 2005, 2005, pp. 155–164.